Available online at www.sciencedirect.com
SCIENCE DIRECT®
Journal of Nuclear Materials 327 (2004) 159–164
journal of nuclear materials
www.elsevier.com/locate/jnucmat

Profile measurements of helium implanted in UO_2 sintered pellets by using the $^3He(d,\alpha)^1H$ nuclear reaction analysis technique

T. Sauvage [a,*], H. Erramli [b], S. Guilbert [a], L. Vincent [a], M.-F. Barthe [a], P. Desgardin [a], G. Blondiaux [a], C. Corbel [c], J.P. Piron [d], F. Labohm [e], A. Van Veen [e]

[a] *Centre d'Etudes et de Recherches par Irradiation, CNRS, 3A, rue de la Ferollerie, 45071 Orléans cedex 2, France*
[b] *Nuclear Physics and Techniques Laboratory, Faculty of Sciences Semlalia, B.P. 2390, University Cadi Ayyad, Marrakech, Morocco*
[c] *Laboratoire de Radiolyse, CEA Saclay, France*
[d] *DEN/DEC/SESC, CEA Cadarache, France*
[e] *Interfaculty Reactor Institute, Delft University of Technology, Mekelweg 15, 2629 JB Delft, The Netherlands*

Received 10 July 2003; accepted 2 February 2004

Abstract

Profiling of ^3He implanted in sintered uranium dioxide pellets was performed using $^3He(d,\alpha)^1H$ Nuclear Reaction Analysis technique. To accurate profile measurements, the cross-section of the $^3He(d,p)^4He$ nuclear reaction was carefully measured with a relative standard deviation of 5%. The total cross-section represented by a fit function is compared with data from literature. With the described coincidence arrangement, we obtained a reduction by a factor $\approx 4\times10^4$ of the signal of deuterons elastically scattered in uranium and a total suppression of parasite signals in the region of helium profiling. This technique enables us to measure helium profile in UO_2 a couple of microns below the surface with a resolution of 0.1 μm and a detection limit of 0.01 at.%.

PACS: 66.30.h; 61.82.m; 81.05.Je

1. Introduction

The detection of helium nearby the surface of solids is of interest in many fields of solid state research (semiconductors, metallurgy, electrochemistry, etc.). Recently, some studies have been devoted to the helium behavior in nuclear materials. Indeed, the principal source of radiation during long term storage of nuclear wastes (glasses or spent fuels) and in matrices for transmutation is α decay of actinides [1–7]. Amounts of helium could be large, and depending on temperature, this can change the chemical and mechanical stability of the materials.

A review of helium detection methods especially based on interactions of energetic charged particles was given by Paszti [8]. Among the reported techniques, the $^3He(d,\alpha)^1H$ Nuclear Reaction Analysis method (NRA) has the highest depth resolution for the detection of α-particles. This technique has been successfully applied for the profiling of ^3He in near-surface layers (<0.3 μm), where the $^3He(d,\alpha)^1H$ cross-section can be considered as constant [9–11]. For larger depth, its sensitivity is deteriorated by the presence of large sources of background. The main sources of interference with the α signal are pulse pileup from high rates of backscattered deuterons,

* Corresponding author. Tel.: +33-2 38 255 419/630 271; fax: +33-2 38 630 271/255 419.
E-mail address: sauvage@cnrs-orleans.fr (T. Sauvage).

0022-3115/$ - see front matter © 2004 Elsevier B.V. All rights reserved.
doi:10.1016/j.jnucmat.2004.02.002

high energy protons emitted from $^3He(d,p)^4He$ and particles emitted from nuclear reactions of other light elements in the target, such as carbon, nitrogen or oxygen.

In the case of $^2H(^3He,\alpha)^1H$ nuclear reaction used for deuterium detection, different techniques have been used to reduce some of these interference sources. Möller [12] used an electrostatic deflector to separate emitted α-particles and backscattered ^3He incident ions, where the backscattered ^3He yield was reduced by a factor of 10^3. This background reduction results in an enhanced sensitivity for deuterium detection. This arrangement is also applicable to ^3He depth profiling by means of the reciprocal $^3He(d,\alpha)^1H$ nuclear reaction, but the suppression of backscattered deuteron signal should be less effective. The coincidence technique, where both reaction products, α-particles and protons, are detected at kinematically corresponding scattering angles, was described by Wielunski and Möller [13]. It provides not only a reduction of the backscattered ^3He intensity by a factor of about 10^3, but also a total suppression of the proton peak.

In the present paper, a similar coincidence technique is applied to the $^3He(d,\alpha)^1H$ nuclear reaction for the ^3He profiling. We describe the coincidence set-up where α-particles and protons are detected in coincidence. The helium profile is extracted from the α energy spectrum by using the reaction cross-section and the energy-range relation for incoming and outgoing particles. To improve the reliability of the concentration calculations, we have measured by using the single and coincidence detection modes the value of the $^3He(d,\alpha)^1H$ cross-section as a function of the incident deuteron energy. There is indeed a large uncertainty in the value at the maximum of the cross-section. It differs by as much as 30% depending on the authors [13–19]. The results obtained by the coincidence technique show that the profile at depth over 1 μm can be resolved at a scale of 0.1 μm with a ^3He detection limit close to 0.01 at.% in ^3He implanted UO_2. Such resolution is impossible to achieve in a standard detection mode, where only the α-particles or protons are detected.

2. Experimental set-up

The deuteron beam is produced by a 3.5 MV Van de Graaff accelerator. The energy calibration has been performed by using $^{27}Al(p,\alpha)^{28}Si$, $^7Li(p,n)^7Be$ and $^{12}C(^3He,n)^{14}O$ reactions with resonances at 991.9, 1880.4 and 1437.9 keV, respectively. A collimator of 0.5×0.5 mm^2 defines a rectangular beam spot on the surface sample. The emitted α-particles from the $^3He(d,\alpha)^1H$ nuclear reaction are detected with a passivated implanted planar silicon (PIPS) detector (25 mm^2 sensitive area, 50 μm depletion layer and energy resolution ≈12 keV) located at an angle of 165° from the beam direction and at a distance of 50 mm from the sample. The solid angle seen by the PIPS detector integrates the αs emitted in the [163°, 167°] angular range. The nuclear reaction kinematics calculations show that for deuteron energy up to 1 MeV the 16.5 MeV protons emitted in coincidence with such αs should be observed at an angle range of 7–14° from the beam direction. Therefore, it is necessary to detect the high-energy protons in transmission geometry through the sample. This detection requires that the sample thickness is lower than the projected range of 16.5 MeV protons in the studied material. For proton detection, a 300 mm^2 PIPS detector with a depletion layer of 300 μm is positioned at the 0° angle from the beam direction and at a distance of 7 mm from the rear surface of the sample. The solid angle of proton detection is considerably larger than required by kinematics to take into account the multiple scattering of αs and protons in the sample. The geometrical arrangement between the α and proton detectors ensures a coincidence efficiency of 100%.

The deuteron incident charge is monitored using a current chopper, previously calibrated with a Faraday cup. The coincidence time between the output signals from the 25 and 300 mm^2 PIPS detectors is 0.4 μs. Energy calibration of the α-particles detector was performed using 1.6 and 2.2 MeV α beams. It is determined from the signals of the backscattered alphas on the polished surface of silicon, nickel and gold samples.

Furthermore, an advantage of our set-up is the high yield of protons detected with the 300 mm^2 PIPS that gives short analysis time to obtain good counting statistics. This would enable us to perform helium cartography of the studied sample with a deuteron microbeam.

3. Cross-section measurements

The ^3He targets used for the determination of the $^3He(d,\alpha)^4He$ cross-section were prepared by ^3He ion implantation into ⟨1 1 1⟩ silicon wafers. ^3He ions were implanted at a target temperature of 300 K with a fluence of 10^{16} $^3He/cm^2$ using a 10 keV $^3He^+$ beam. The beam was scanned to obtain homogeneous implantation and the wafer of 600 μm thickness and of 2 in. diameter was mounted 6° off axis in order to avoid significant channeling effects. At an energy of 10 keV, the SRIM simulation [20] gives that the depth at the maximum ^3He concentration is 130 nm with a full-width at half-maximum (FWHM) of the ^3He distribution close to 150 nm. Three 1 cm^2 samples have been cutted from the implanted silicon wafer. The ^3He fluence of each sample has been measured by the $^3He(n,p)^3H$ neutron depth profiling (NDP) technique at Delft University of Technology (IRI) with an international standard. The mean value is 9.5×10^{15} $^3He/cm^2$ with a standard deviation of

2.5%. The fluence measured by NDP technique is in good agreement with the implantation fluence.

We measured the cross-section from the peak area of αs or protons. The αs are detected at 165° in coincidence with protons in the above mentioned geometry. The protons detection is performed with a Si(Li) detector (25 mm^2 sensitive area, 5000 μm depletion layer, 30 μm aluminum filter) mounted at 0° and 165° with a distance from the sample of 43 mm. The initial energy of the deuteron beam is varied in the 322–1000 keV range. The use of the implantation technique to obtain the ^{3}He standard needs to correct the incident deuteron energy value. At the depth of 130 nm, the 322–1000 keV range corresponds to an energy range between 307 and 992 keV for which the ^{3}He(d, p)^{4}He differential cross-section is measured (Fig. 1).

The energy standard deviation of the individual data is calculated by considering the ^{3}He gaussian depth distribution into the standard. It is estimated to the difference of the mean deuteron energy calculated by SRIM at the (Rp ± FWHM) depth values. For example, the energy standard deviation is 16 keV and 8 keV for incident deuteron energy of 300 and 1000 keV, respectively. At the depth of 130 nm, the beam straggling is close to 1.5 keV and consequently is considered as negligible in the evaluation of the energy standard deviation. The cross-section standard deviation is given by the quadratic sum of the standard deviations of the solid angle (2%), the incident charge (2%), the peak area (2–5%) and the ^{3}He implantation fluence of the sample (2.5%). As expected, the data obtained with the single and coincidence detection modes are in good agreement. The precision of the cross-section data is close to 5%.

Yarnell et al. [16] reports that $(d\sigma/d\Omega)_{c.m}$ is isotropic below 500 keV. For higher energies, low angular dependence of the ^{3}He(d, p)^{4}He cross-section is observed by Yarnell et al. [16] and Bonner et al. [17]. They reported that the ratio of the proton yield detected at 0° by the proton yield obtained at 90° amounts to 1.07 and 1.04 for incident energy of 978 and 1140 keV, respectively. Since the anisotropy is low at energies below 1 MeV, the differential cross-section multiplied by 4π or total cross-sections determined in this work can be compared with data determined in different geometry (Fig. 2). The energy corresponding to the maximum cross-section is 418 keV and agrees with that reported by Moller and Besenbacher [14], by Yarnell et al. [16] and by Bonner et al. [17]. Comparing the cross-section values obtained in this work with the literature data, one can notice that, except data reported by Bonner, the discrepancy is characterized by a relative uncertainty of 7–14% at the cross-section maximum and of 2–10% at higher energies.

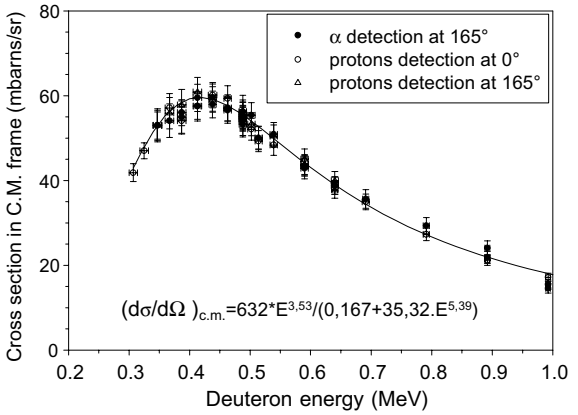

Fig. 1. Differential cross-section in the center-of-mass frame $(d\sigma/d\Omega)_{c.m.}$ for ^{3}He(d, p)^{4}He nuclear reaction at different laboratory angles.

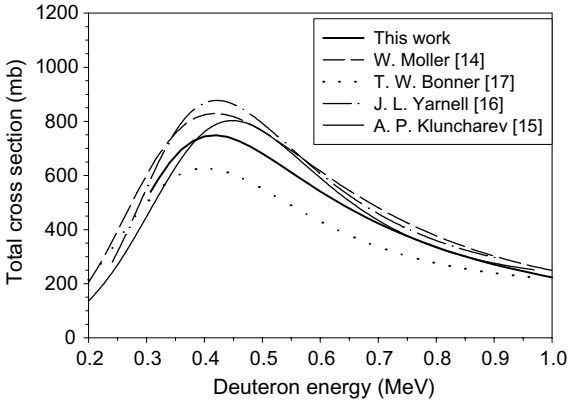

Fig. 2. Comparison of total cross-section of the ^{3}He(d, p)^{4}He nuclear reaction measured by different authors.

In contrast of the data of Yarnell [16], Bonner [17] and Kluncharev [15] obtained in the fifties, this work is performed with today's modern experimental equipment (current chopper, semiconductor detector, energy calibration of the accelerator, etc.). The large experimental error in the previous references can be attributed to the use of ^{3}He or ^{2}H gas-target.

The ratio between data of this work and Moller is constant as a function of the incident energy. This systematic error could be connected with the determination of the charge (current chopper for this work and gold marker for Moller), with the inaccuracy of the ^{2}H or ^{3}He implantation fluence of the standard of Moller, with some possible spectral interference.

4. Depth profile of helium implanted in UO_2 sintered pellets

Two sintered uranium dioxide disks (0.2 at.% ^{235}U) have been used to study the potentialities of the

technique of coincidence detection of the emitted products for ^{3}He profiling in large depth. The mean grain size is 8 μm and the mean O/U ratio is 2.0083 ± 0.0060. The density of the material is 10.46 ± 0.03 g/cm^3. The disks are 300 μm thick and 8 mm in diameter. This thickness enables the detection of protons through the disk at 0°.

The UO_2 disks have been implanted with 1 MeV ^{3}He using the 3.5 MV Van de Graaff accelerator at CERI Orléans. The implantation is performed by focusing the beam (1×1 mm^2) and by sweeping it over the disk surface to ensure a homogeneous dose. Both disks have been implanted with the same flux, at two different fluences: 10^{16} for the first disk and 5×10^{16} ^{3}He/cm^2 for the second. The corresponding implantation depth calculated by SRIM 2000 is 2.0 μm. To optimize the sensitivity of the ^{3}He analysis, the deuteron incident energy was fixed at 768 keV. At the depth of 2 μm, the mean energy of deuteron is 470 keV, which almost corresponds to the maximum of the (d, α) cross-section. These conditions allow to probe ^{3}He in UO_2 up to the maximum depth of 3.5 μm.

Fig. 3 shows experimental spectra of 5×10^{16} ^{3}He/cm^2 implanted UO_2 disk acquired with the 25 mm^2 PIPS detector at 165° in single and coincidence detection mode. The beam current is 8 nA to limit to 3% the dead time of the nuclear electronics and in the same time to reduce the accidental coincidence rate. We can notice that in the single mode spectrum the $^3He(d, \alpha)^1H$ peak which should be around the channel 340 is masked whereas in the coincidence mode this peak can be easily distinguished. In the coincidence mode, the intensity of the backscattered deuterons is reduced by a factor of about 4×10^4 (Fig. 3). In the $[100, 600]$ channel range, the pile-up signal from $U(d, d)$ elastic reaction and the signals of protons emitted from the $^{16}O(d, p_1)^{17}O$ and $^{16}O(d, p_0)^{17}O$ nuclear reactions are consequently suppressed. The background being close to zero, this technique makes possible the measurement of helium profile in case of implantation depth at micrometric scale with a limit detection of 10^{15} ^{3}He/cm^2.

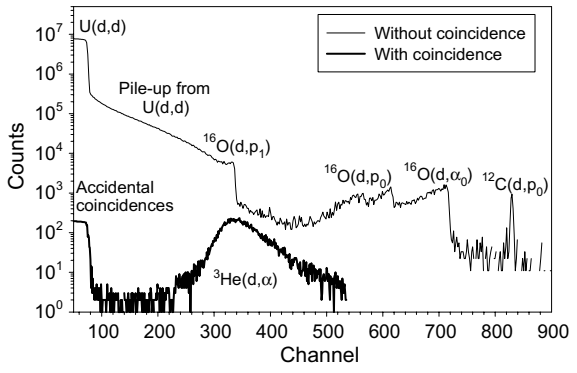

Fig. 3. Energy spectra in single and coincidence mode at 165° for UO_2 sintered disks implanted with 5×10^{16} ^{3}He/cm^2 at 1 MeV. Analysis were performed with 768 keV D^+ ions at 8 nA, and at a total charge of 250 μC.

To determine the ^{3}He depth profile, the experimental spectrum performed in coincidence detection mode is fitted by using the SIMNRA program, in which the measured $^3He(d, \alpha)^4He$ cross-section and the stopping powers of Ziegler [20] are integrated. This program fits the experimental data assuming a sequence of uranium dioxide layers with different ^{3}He concentrations. The experimental spectrum and its fit are shown in Fig. 4a for the 5×10^{16} ^{3}He/cm^2 implanted disk. The ^{3}He profile used to obtain the fit is presented in Fig. 4(b). Several experimental spectra have been acquired at different target regions in the both disks implanted at 10^{16} and 5×10^{16} ^{3}He/cm^2. The deduced ^{3}He profiles are shown in Fig. 5. One can notice the good reproducibility of the profile measurement. Table 1 lists the determined fluence, the ^{3}He maximum concentration $[He]_{max}$, the depth at $[He]_{max}$ and the full width at half maximum (FWHM) of the profiles. These values have been determined with

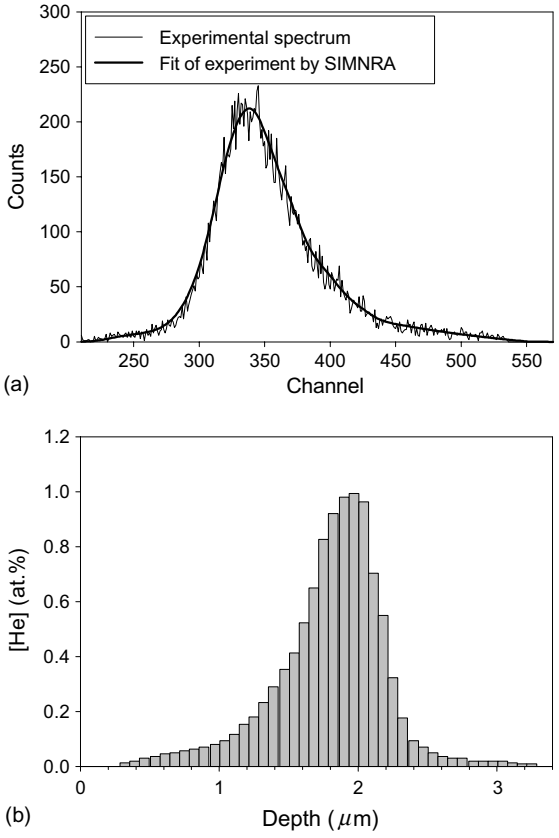

Fig. 4. Experimental spectrum of the sample implanted with 1 MeV ^{3}He at 5×10^{16} ^{3}He/cm^2 and its fit by SIMNRA (a) and He profile used for the fit (b). Analysis were performed with 768 keV D^+ ions at 8 nA, and at a total charge of 250 μC.

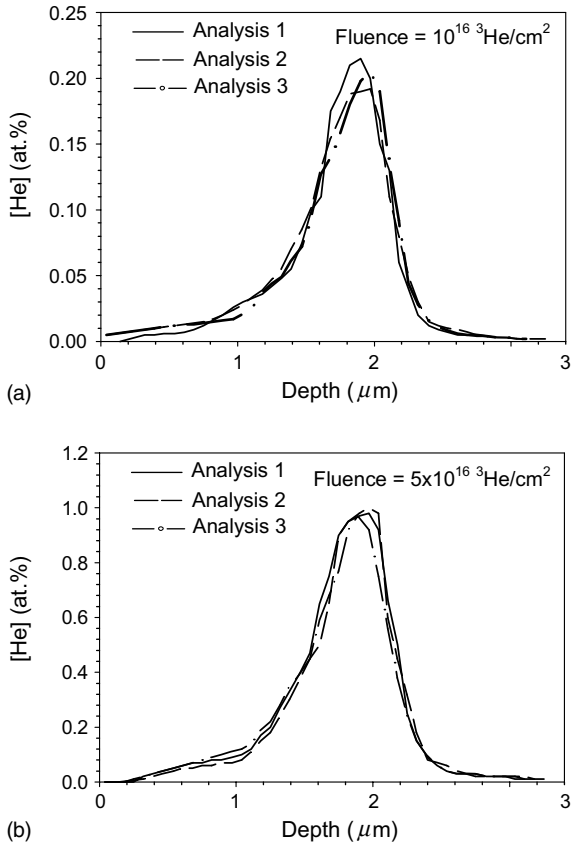

Fig. 5. ^{3}He profiles determined in the UO_2 disks implanted at 1 MeV with 10^{16} (a) and 5×10^{16} ^{3}He/cm^2 (b) fluences.

Table 1
Measured fluence, ^{3}He maximum concentration $[He]_{max}$, depth at $[He]_{max}$ and full width at half maximum (FWHM) from ^{3}He profile determined in UO_2 samples implanted at 1 MeV with 10^{16} and 5×10^{16} ^{3}He/cm^2

Implantation fluence (10^{16} ^{3}He/cm^2)	1	5
Measured fluence (10^{16} ^{3}He/cm^2)	1.06 ± 0.05	5.19 ± 0.16
$[He]_{max}$ (at.%)	0.20 ± 0.01	1.00 ± 0.03
Depth at $[He]_{max}$ (μm)	1.91 ± 0.04	1.90 ± 0.06
FWHM (μm)	0.60 ± 0.04	0.58 ± 0.03

The experimental standard deviation is calculated from the results of three profiles.

a very good accuracy of about 5% confirming the reproducibility of the measurements. The fluences calculated from the profiles are 1.06×10^{16} and 5.19×10^{16} ^{3}He/cm^2 and then in excellent agreement with those obtained by charge measurements. This outlines the accuracy of the cross-section measurements and the charge integration during the implantation and the analysis. Depths at $[He]_{max}$ and FWHM are similar at both implantation fluences and the ratio of the ^{3}He maximum concentration (5.0 ± 0.3) is close to the fluence ratio (4.9 ± 0.3).

The main factor affecting the ^{3}He detection sensitivity is the presence of background. With the coincidence technique, the level of counts underlying the region of interest is zero. The detection sensitivity can be defined as one count per channel. In the above mentioned conditions of analysis, SIMNRA calculations reveal that this yield corresponds to 0.01% ^{3}He atomic concentration into the bulk.

Depth resolution is dependent to the kinematics of the nuclear reaction, the probing depth and the stopping power of the detected particles. Detection of the emitted α-particles allows us to get a resolution five times better than the one obtained by the detection of protons emitted at high energy. The minimum detectable depth difference estimated from calculations with SIMNRA is 0.03 μm in the near surface and 0.1 μm for probing depth close to 2 μm.

The experimental ^{3}He profile of the sample implanted at 5×10^{16} ^{3}He/cm^2 is compared to SRIM 2000 calculations in Fig. 6. The maximum of ^{3}He concentration is measured at a depth of 1.9 μm. This value is in good agreement with the most probable projected range calculated by SRIM ($R_p\approx2$ μm). The ^{3}He experimental maximum concentration (1 at.%) is lower than the one calculated by SRIM (1.4 at.%). The experimental full-width at half-maximum is larger than the one calculated by SRIM (0.6 μm versus 0.45 μm). It is worth noting the presence of a large helium tail between the surface and the implantation depth for both implantation fluences. Among the processes which may be proposed to explain such a He tail, we investigated the effect of deuteron analysis on He diffusion. We determined the He profile

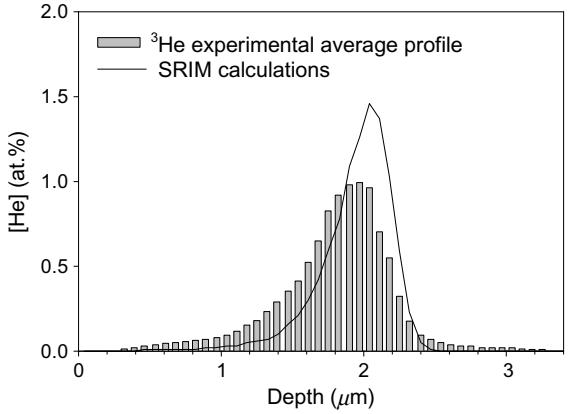

Fig. 6. ^{3}He profile in UO_2 disk implanted at 1 MeV with 5×10^{16} ^{3}He/cm^2 determined by the ^{3}He(d, α)^{1}H nuclear reaction method and compared with SRIM calculations.

in the 10^{16} ^{3}He/cm^2 implanted disk from the sum of eight experimental spectra acquired at different position with a deuteron charge reduced at the eighth of the one used in the typical analysis conditions, it means 12.5 μC. The He profile determined in these conditions is comparable to the one obtained at the typical analysis deuteron charge of 100 μC. It suggests that the He tail observed between the surface and the implantation peak is not due to the high deuteron fluence needed to obtain good counting statistics. Let's notice that the reduced 12.5 μC charge used in these last experiments corresponds to a deuteron fluence of 2×10^{16} at/cm^2 which is of the same order as the ^{3}He implanted one. However the deuteron flux is 300 times lower than the ^{3}He one used during implantation. This suggests that if He diffusion occurs during irradiation the effect of the deuteron analysis should be lower than the one of the implantation. Indeed the heating induced by the implantation can be the source of the ^{3}He diffusion and of this tail. In our irradiation set-up where the sample is not cooled, the temperature measured on the sample holder is lower than 120 °C. Of course, this measurement gives any indication on the real temperature of the target. In future, a sample cooling integrated in the implantation chamber and some implantations at low flux will enable to give some conclusions about the eventual ^{3}He diffusion during implantation. The well known underestimating of the straggling by SRIM can be also the source of discrepancy between calculated and experimental He profile.

5. Conclusion

In this study, we investigated the coincidence detection of protons and α-particles emitted from the ^{3}He(d, p)^{4}He nuclear reaction to profile He at micrometric depth in sintered UO_2 pellets. The ^{3}He(d, p)^{4}He cross-section was measured with single and coincidence modes. These cross-section values have been used to determine ^{3}He depth profiles of high energy ^{3}He implanted in sintered uranium dioxide pellets. The measured and the implanted fluences are in good agreement. In case of micrometric implantation depth, the coincidence detection technique allows to reach a resolution of 0.1 μm with a detection limit close to 0.01 at.%. This technique will allow us to study the evolution of the depth profile of ^{3}He in UO_2 after thermal annealing. The detection technique of high energy protons emitted to 0° and detected in transmission through the sample will become in near future an essential tool to study by means of micro-cartography the role of grain boundaries in the helium diffusion in UO_2.

Acknowledgements

The authors are grateful to the French electrical utility Électricité de France (EDF) and the Research Program on the long term Evolution of Spent Fuel waste Packages of the CEA (PRECCI) for their financial support.

References

[1] R. Fromknecht, J.-P. Hiernaut, H.J. Maztke, T. Wiss, Nucl. Instrum. and Meth. B 166–167 (2000) 263.
[2] D. Gosset, P. Trocellier, Y. Serruys, J. Nucl. Mater. 303 (2002) 115.
[3] E.A.C. Neeft, R.P.C. Schram, A. Van Veen, F. Labohm, A.V. Fedorov, Nucl. Instrum. and Meth. B 166–167 (2000) 238.
[4] E.A.C. Neeft, A. Van Veen, R.P.C. Schram, F. Labohm, Progr. Nucl. Energy 38 (3–4) (2001) 287.
[5] S. Ouchani, J.-C. Dran, J. Chaumont, Appl. Geochem. 13 (6) (1998) 707.
[6] S. Ouchani, J.-C. Dran, J. Chaumont, Nucl. Instrum. and Meth. B 132 (1997) 447.
[7] He Zhiyong, P. Jung, Nucl. Instrum. and Meth. B 166–167 (2000) 165.
[8] F. Pàszti, Nucl. Instrum. and Meth. B 66 (1992) 83.
[9] W. Jäger, J. Roth, Nucl. Instrum. and Meth. 182&183 (1981) 975.
[10] B.M.U. Scherzer, H.L. Bay, R. Behrisch, P. Børgesen, J. Roth, Nucl. Instrum. and Meth. 157 (1978) 75.
[11] R. Schultz, R. Behrisch, B.M.U. Scherzer, Nucl. Instrum. and Meth. 168 (1980) 295.
[12] W. Möller, Nucl. Instrum. and Meth. 157 (1978) 223.
[13] M. Wielunski, W. Möller, Nucl. Instrum. and Meth. B 50 (1990) 23.
[14] W. Möller, F. Besenbacher, Nucl. Instrum. and Meth. 168 (1980) 111.
[15] A.P. Kluncharev, B.N. Eselson, A.K. Valter, Doklady Academii Nauk SSSR 109 (1956) 737.
[16] J.L. Yarnell, R.H. Lovberg, W.R. Stratton, Phys. Rev. 90 (1953) 292.
[17] T.W. Bonner, J.P. Conner, A.B. Lillie, Phys. Rev. 88 (1953) 473.
[18] H.-S. Bosch, G.M. Hale, Nucl. Fusion 32 (4) (1992) 611.
[19] C.J. Altstetter, R. Behrisch, J. Bøttiger, F. Pohl, B.M.U. Scherzer, Nucl. Instrum. and Meth. 149 (1978) 59.
[20] J.F. Ziegler, J.P. Biersack, U. Littmark, The Stopping and Range of Ions in Matters, Pergamon, New York, 1985.